

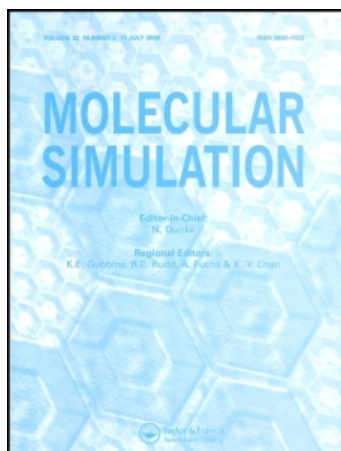
This article was downloaded by: [University of Minnesota Library]

On: 23 October 2008

Access details: Access Details: [subscription number 782638545]

Publisher Taylor & Francis

Informa Ltd Registered in England and Wales Registered Number: 1072954 Registered office: Mortimer House, 37-41 Mortimer Street, London W1T 3JH, UK



## Molecular Simulation

Publication details, including instructions for authors and subscription information:

<http://www.informaworld.com/smpp/title-content=t713644482>

### Accurate computation of shear viscosity from equilibrium molecular dynamics simulations

D. Nevins<sup>a</sup>; F. J. Spera<sup>a</sup>

<sup>a</sup> Department of Earth Science, University of California, Santa Barbara, CA, USA

Online Publication Date: 01 December 2007

**To cite this Article** Nevins, D. and Spera, F. J.(2007)'Accurate computation of shear viscosity from equilibrium molecular dynamics simulations',Molecular Simulation,33:15,1261 — 1266

**To link to this Article:** DOI: 10.1080/08927020701675622

**URL:** <http://dx.doi.org/10.1080/08927020701675622>

PLEASE SCROLL DOWN FOR ARTICLE

Full terms and conditions of use: <http://www.informaworld.com/terms-and-conditions-of-access.pdf>

This article may be used for research, teaching and private study purposes. Any substantial or systematic reproduction, re-distribution, re-selling, loan or sub-licensing, systematic supply or distribution in any form to anyone is expressly forbidden.

The publisher does not give any warranty express or implied or make any representation that the contents will be complete or accurate or up to date. The accuracy of any instructions, formulae and drug doses should be independently verified with primary sources. The publisher shall not be liable for any loss, actions, claims, proceedings, demand or costs or damages whatsoever or howsoever caused arising directly or indirectly in connection with or arising out of the use of this material.

# Accurate computation of shear viscosity from equilibrium molecular dynamics simulations

D. NEVINS\* and F. J. SPERA

Department of Earth Science, University of California, Santa Barbara, CA 93106, USA

(Received 29 September 2006; in final form 10 September 2007)

The accuracy of the Green–Kubo formulation for computing shear viscosity from equilibrium molecular dynamics simulations depends on the quality of the potential and on how the viscosity computation is carried out. We examine the role of the duration of the simulation, the number of particles used, and how the correlations are accumulated on the accuracy of the computed viscosity. We propose as a measure of the accuracy the standard deviation of five independently computed shear viscosity values based on independent components of the stress tensor. Using this measure, we examine the shear viscosity calculation for molten NaCl to determine the values of the run length, window width, and spacing between windows and obtain a good compromise between calculation time and viscosity quality. Significantly we note that even though viscosity can be calculated using relatively few particles, reducing state point uncertainty requires more, rather than less, particles.

*Keywords:* Viscosity; Molecular dynamics; NaCl; Green–Kubo

## 1. Introduction

Some of the methods for computing shear viscosity include Enskog theory [1], non-equilibrium molecular dynamics (NEMD), the Stokes–Einstein equation, and the Green–Kubo expression [2]. The Green–Kubo (GK) expression for the shear viscosity is given by integration of the stress (pressure) autocorrelation function. In particular, the shear viscosity is computed according to

$$\eta = \frac{V}{3k_B T} \int_0^\infty \left\langle \sum_{x < y} P_{xy}(t) P_{xy}(0) \right\rangle dt \quad (1)$$

where  $\eta$  is the shear viscosity,  $V$  is the volume of the system,  $T$  is the temperature,  $k_B$  is Boltzmann's constant, and  $P_{xy}$  refers to the  $xy$  component of the stress. The GK formulation utilizes a single summation that consolidates the contributions of all the atoms into a single autocorrelation function

$$C_{xy}(t) = \left\langle \sum_{x < y} P_{xy}(t) P_{xy}(0) \right\rangle. \quad (2)$$

This allows the formulation to be used with molecular dynamics simulations whereas alternative formulations based on particle displacement require translational invariance, an assumption violated in MD simulations utilizing periodic boundary conditions. The angle brackets around the summation in equation (2) refer to an average of a 'sufficiently large' number of samples [3]. Four other independent estimates of the shear viscosity can be computed from the remaining off-diagonal and normal components of the stress  $P_{xz}$ . To study the optimal way to implement equation (1), it is useful to refer to specific quantities illustrated schematically in figure 1. These quantities include the duration of the MD simulation,  $t_D$ , the time 'window' over which the autocorrelation  $C(t)$  is computed,  $t_W$ , and the time interval between the start of successive time windows,  $t_S$ . These quantities are related to each other and the number of time origins,  $n_O$ , used in the summation according to

$$n_O = 1 + \left[ \frac{t_D - t_W}{t_S} \right] \quad (3)$$

where the operation implied by the square brackets returns the integer part of the quotient. Since for GK computation of viscosity,  $t_D$  is of order a few ns, and  $t_W$  is a few ps,  $n_O$

\*Corresponding author. Email: dean@nevins.org

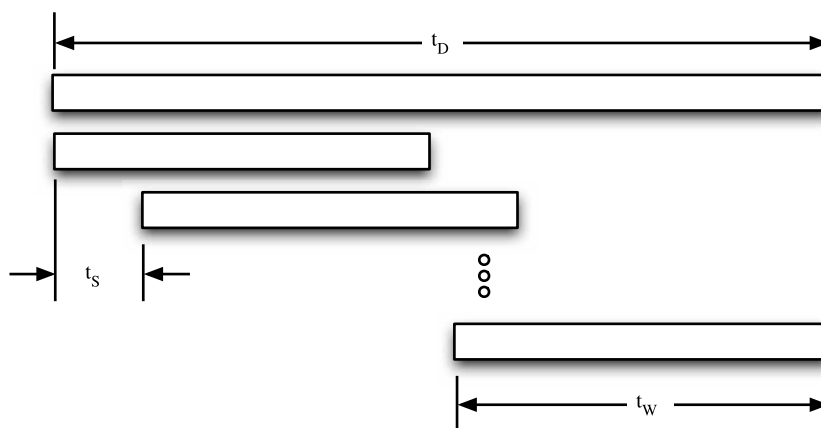


Figure 1. Schematic diagram illustrating the relationship between the time intervals used to compute the shear viscosity from MD simulation data using the Green–Kubo formulation.  $t_D$  refers to the total duration of the simulation. The autocorrelation functions for the stress components  $P_{xy}$ ,  $P_{xz}$ ,  $P_{yz}$ ,  $P_{xx} - P_{yy}$  and  $P_{yy} - P_{zz}$  are each partitioned into multiple windows of duration  $t_W$  and have their origins separated from one another by  $t_S$ . The number of time origins (equal to the number of windows) is given exactly by equation (3) and approximately by equation (4).

reduces to

$$n_O = n_W \approx \left[ \frac{t_D}{t_S} \right] \quad (4)$$

In this investigation we determine the dependence of the shear viscosity on  $t_D$ ,  $t_S$  and  $t_W$  and  $N$ , the number of particles used in the simulation, in order to deduce the most efficient and accurate method for computation of the shear viscosity by the Green–Kubo formulation. In order to gauge the effects of simulation duration, window width and number of origins on the precision of the viscosity, a measure of the error of the viscosity is introduced. We exploit the fact that each of the five independent components of the stress tensor (i.e.,  $P_{xy}$ ,  $P_{xz}$ ,  $P_{yz}$ ,  $P_{xx} - P_{yy}$ , and  $P_{yy} - P_{zz}$ ) provides an independent estimate of the shear viscosity. We define the fractional error,  $\xi$ , as the root mean square of the ‘component’ deviations from the average shear viscosity,  $\eta_{AVE}$ , divided by the average viscosity according to

$$\xi = \frac{1}{\eta_{AVE}} \sqrt{\frac{(\eta_{xy} - \eta_{AVE})^2 + (\eta_{xz} - \eta_{AVE})^2 + (\eta_{yz} - \eta_{AVE})^2 + (\eta_{xx} - \eta_{yy} - \eta_{AVE})^2 + (\eta_{yy} - \eta_{zz} - \eta_{AVE})^2}{5}} \quad (5)$$

where  $\eta_{AVE}$  is the arithmetic mean of the five independently determined viscosity estimates  $\eta_{xy}$ ,  $\eta_{xz}$ ,  $\eta_{yz}$ ,  $\eta_{xx}$  and  $\eta_{yy}$ .

The accuracy of the shear viscosity in the sense of comparison with laboratory values depends obviously on the quality of the potential. Here we study molten NaCl because it is a simple material for which an accurate effective pair potential exists. Although the point of this investigation is not to find a better description of the pair potential applicable to NaCl, it is informative to compare

MD computed values with laboratory data [5]. The methodology developed in this study is directly applicable to determination of shear viscosity in other materials including molten geoliquids at conditions of elevated temperature (2000–5000 K) and pressure (0–135 GPa) relevant to geophysical studies of the earth’s partially molten interior.

## 2. Model and simulation parameters

For this investigation, NaCl was simulated using the potential form

$$\phi_{ij}(r_{ij}) = \frac{q_i q_j}{r_{ij}} + A_{ij} \exp\left(\frac{-r_{ij}}{B_{ij}}\right) - \frac{C_{ij}}{r^6} - \frac{D_{ij}}{r^8} \quad (6)$$

This form has been shown to describe the alkali halides quite well [6–8]. The numerical values of the parameters used are given in table 1. The MD code utilized was a modified version of the Large-scale Atomic/Molecular Massively Parallel Simulator (LAMMPS) [9]. The pair potential has contributions from Coulombic forces, Born–Mayer exponential electron repulsion (table 1), dipolar and quadrupolar terms. Long-range Coulomb terms were computed using the Particle–Particle Particle–Mesh K-space solver with a precision of one part in 10,000. Short-range Coulombic interactions, Born–Mayer repulsions, and dipolar and quadrupolar forces are calculated directly within a 0.6 nm (6 Å) radial cutoff in direct space.

The simulations were carried out in the NEV (microcanonical ensemble) with the numbers of particles

Table 1. Potential parameters for NaCl used in this study.

Species	$A_{ij} (\times 10^{-7} \text{ J mol}^{-1})$	$B_{ij} (\times 10^{11} \text{ m})$	$C_{ij} (\times 10^{52} \text{ J m}^6 \text{ mol}^{-1})$	$D_{ij} (\times 10^{73} \text{ J m}^8 \text{ mol}^{-1})$
Na–Na	4.040947	3.174603	1.011070	4.814617
Na–Cl	11.948257	3.174603	6.740466	83.653976
Cl–Cl	33.120536	3.174603	69.811965	1402.257558

ranging from 258 to 25,800. Ion positions are updated using the leapfrog Verlet scheme with a timestep of 1 femtosecond (fs). Initial conditions were developed using the skew-start methodology [10] with an initial temperature distribution of 5000 K. Upon removal of net momentum, temperature was held to 5000 K by velocity scaling for 10 ps. The system was cooled from 5000 K to the target temperature of 1400 K using the “slow” cooling schedule ( $0.5 \times 10^{13} \text{ K s}^{-1}$ ) adopted by Matsui and Kawamura [11]. The liquid was then held at 1400 K for 150 ps to achieve thermal equilibrium by velocity scaling. At thermal equilibrium, velocity scaling was turned off and production runs of duration  $t_D$  2–10 ns were carried out. Potential and kinetic energy, temperature, isochoric heat capacity and the stress components  $P_{xx}$ ,  $P_{yy}$ ,  $P_{zz}$ ,  $P_{xy}$ ,  $P_{xz}$  and  $P_{yz}$  were computed and saved every timestep.

For  $N = 25,800$  particles (12,900 NaCl ‘molecules’) at  $1379.3 \text{ kg m}^{-3}$  and using  $t_D = 2 \text{ ns}$ ,  $t_W = 2 \text{ ps}$ , and  $t_S$  of 10 fs, the simulated temperature was  $1410 \pm 19 \text{ K}$ . Pressure was  $197.6 \pm 21.0 \text{ MPa}$  and the viscosity was  $0.692 \text{ MPa s}$ . This compares favourably with the laboratory results for NaCl summarized extensively by Janz [5] who reports a density of  $1377.6 \text{ kg m}^{-3}$  and a viscosity of  $0.614 \text{ MPa s}$  at 1400 K and 0.1 MPa. Our slightly higher computed density is consistent with the higher pressure of the MD simulation compared to the laboratory measurement.

### 3. Results and discussion

#### 3.1 Selection of window width ( $t_W$ )

When computing the autocorrelation function  $C(t)$ ,  $t_W$  (figure 1) must be chosen.  $t_W$  should be long enough to

capture the decay of  $C(t)$  in its entirety but not so long that the noise added to the correlation signal contaminates the intrinsic value of the stress autocorrelation function. Figure 2 shows a typical autocorrelation  $C(t)$  for the off-diagonal pressure  $P_{xy}$ .  $C(t)$  decays rapidly towards zero and, after about 1 ps,  $C(t)$  exhibits small amplitude oscillations around zero (figure 2). The rate of the descent toward zero differs for each of the autocorrelations and for each run. We have chosen to cut off the contribution of  $C(t)$  at the time step where the slowest decaying  $C(t)$  functions falls below 0.005. In practice, this value varied from about 0.56–1.35 ps. In order to have a uniform window width, a conservative value of 2 ps is adopted and used throughout the rest of this study.

#### 3.2 Role of simulation duration ( $t_D$ )

To examine the effects of changing run duration  $t_D$  on computed viscosity, the window width ( $t_W$ ) and spacing ( $t_S$ ) were set equal to 2 ps and 0.01 ps, respectively. The number of windows and the simulation duration are linked through equation (2) and are not independent at fixed  $t_S$ . Figure 3 shows the variation of  $\xi$ , the fractional error defined by equation (5) plotted against  $t_D$ . The average deviation in the  $t_D$  interval 20–100 ps is  $\approx 25\%$  whereas for the longest simulation duration (10 ns), the deviation is  $< 5\%$ . Simulations of durations of less than  $\sim 1.0 \text{ ns}$  generate significant differences in viscosity values from each autocorrelation and are consequently unsuitable for determining of viscosity. Alternatively, not much additional reduction in  $\xi$  occurs for durations greater than about 2 ns, although the computation time increases considerably. The effect of the run duration,  $t_D$ , is also

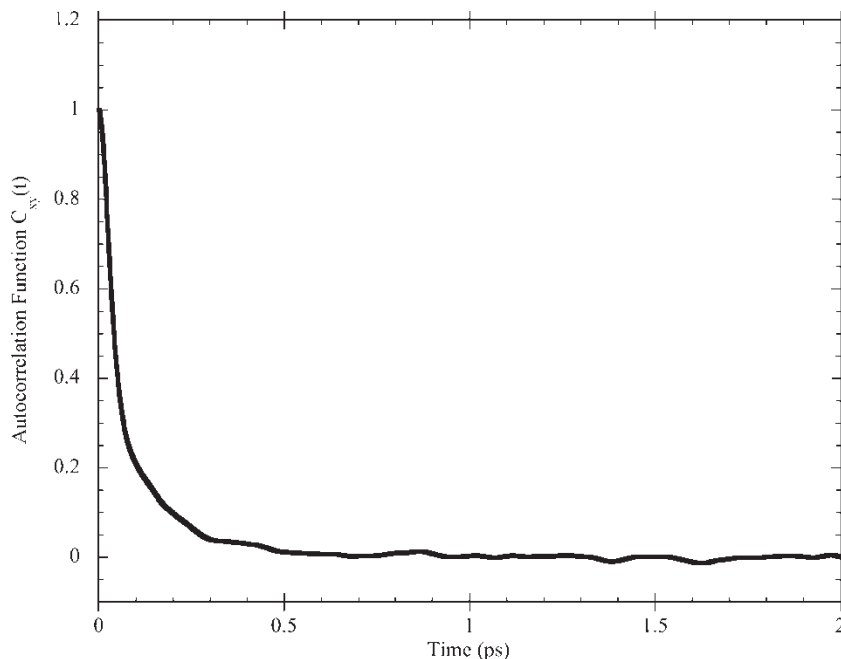


Figure 2. Off-diagonal stress autocorrelation function  $C_{xy}(t)$  vs. time for  $N = 2580$  particles at  $1418 \text{ K} (\pm 18 \text{ K})$ ,  $202.9 \text{ MPa} (\pm 46.6 \text{ MPa})$  and density of  $1379.3 \text{ kg m}^{-3}$ .

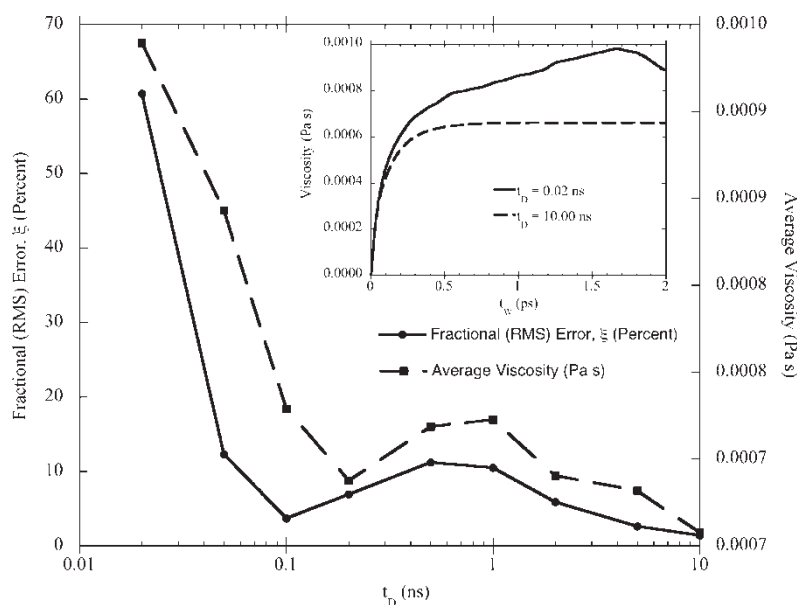


Figure 3. Fractional RMS error,  $\xi$  and component-averaged shear viscosity,  $\eta_{\text{AVE}}$  for 12,960 particles ( $N = 12\,960$ ) at 1424 K ( $\pm 17$  K), 175.8 MPa ( $\pm 24.6$  MPa) and  $\rho = 1379.3 \text{ kg m}^{-3}$  for simulation durations  $t_D$  ranging from 0.02 to 10 ns. A simulation duration  $t_D = 2$  ns is a good compromise between accuracy and computational cost. The inset shows that asymptotic shear viscosity values are not obtained in short duration experiments.

apparent in the value of the average viscosity. As shown in the inset to figure 3, the average viscosity computed for the short duration  $t_D = 0.02$  ns run does not approach an asymptotic limit like the viscosity value computed for  $t_D = 10$  ns. In summary, the combination of a stable  $\eta_{\text{AVE}}$  combined with small  $\xi$  suggests a run length of  $\sim 2$  ns is a good compromise between accuracy and computational cost. In terms of  $n_O$ , the number of origins,  $t_D = 2$  ns corresponds to 200,000 time origins (windows) when the interval between successive windows ( $t_S$ ) is 0.01 ps.

### 3.3 Role of temporal spacing between time origins ( $t_S$ )

In order to test the effect of changing  $t_S$ , the interval between successive time origins on the fractional error  $\xi$ , a series of simulations was carried out at constant  $t_D = 10$  ns. The window spacing  $t_S$  was varied from 1 fs to 100 ps. From equation (4) it is clear that at const  $t_D$ , the number of time origins ( $n_O$ ) is not independent of the window spacing,  $t_S$ .

Figure 4 shows that to obtain  $\xi < 2\%$  the window spacing must be  $t_S$  smaller than  $\sim 100$  fs. Smaller values do not lead to any reduction in  $\xi$ . A value of  $t_S = 10$  fs is a good choice to maintain a small error,  $\xi$ , while minimizing computational time.

### 3.4 Role of system size (particle number)

It has been claimed [4] that increasing the numbers of particles ( $N$ ) has no effect on improving the quality of the Green–Kubo shear viscosity calculation. We have tested this by studying the effect of varying  $N$  at fixed values of  $t_D$  (10 ns),  $t_W$  (2 ps) and  $t_S$  (10 fs). The relationship

between fractional error,  $\xi$  and particle number is depicted in figure 5.

Indeed, there is no correlation between  $N$  and  $\xi$ .  $N$  varies by a factor of 100 from  $N = 258$  to 25,800 and there is no systematic improvement (decrease) in  $\xi$ . The same effect is seen for the average viscosity; increasing  $N$  does give rise to asymptotic behaviour in  $\eta_{\text{AVE}}$ . Although tempting to conclude that increasing  $N$  has little effect on the computed viscosity value, this conclusion is not warranted. The reason is the as follows. It is well known [12] that the fluctuations in pressure ( $\sigma_P$ ) and temperature ( $\sigma_T$ ) during a NEV MD simulation scale as  $N^{-1/2}$ . This is shown in figure 6 by plotting  $\sigma_T/\hat{T}$ , the temperature fluctuation ( $\sigma_T$ ) divided by the mean temperature  $\hat{T}$  of the run, and the analogous quantity for pressure,  $\sigma_P/\hat{P}$ , against  $N$ . It is clear from figure 6 that the uncertainty in temperature and pressure of an MD simulation depends on  $N$  as expected. For example, for  $N = 500$  particles the temperature and pressure of the simulation are known to within 3 and 50%, respectively. For a simulation carried out at a typical geophysically relevant state point of, say, 3500 K and 10 GPa, the uncertainties in temperature and pressure are  $\pm 100$  K and  $\pm 4.8$  GPa, respectively. The large uncertainty in pressure renders almost meaningless any attempt to determine the equation of state for a high-pressure geomaterial, for example. In contrast, a simulation with  $N = 10,000$  particles at the same state point carries with it an error in temperature and pressure of  $\pm 45$  K and  $\pm 1$  GPa, respectively. Because there is a one-to-one mapping between a state point and the shear viscosity, simulations run with large  $N$  are clearly superior than those with small  $N$  since the uncertainties of the state point are smaller in the former than in the latter case.

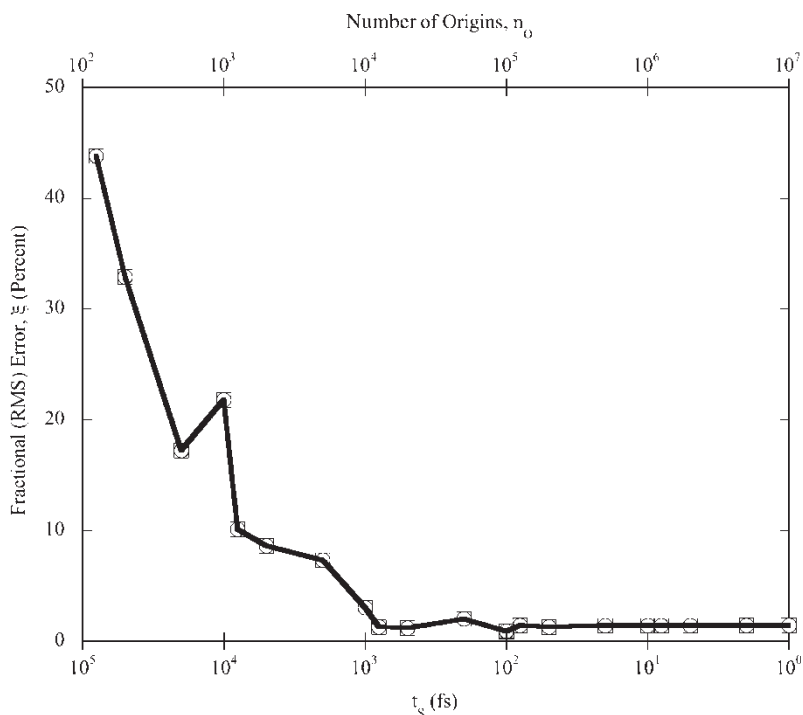


Figure 4. Fractional RMS error,  $\xi$  for  $N = 12,960$  at  $1424 \text{ K} (\pm 17 \text{ K})$ ,  $175.8 \text{ MPa} (\pm 24.6 \text{ MPa})$  and  $\rho = 1379.3 \text{ kg m}^{-3}$  vs. the number of time origins ( $n_o$ ) or the time spacing,  $t_s$ , between successive time origins used in calculation of the autocorrelation function. At least 100,000 origins or ( $t_s = 10 \text{ fs}$ ) are needed to develop adequate statistics for determination of shear viscosity. Run duration is  $t_D = 10 \text{ ns}$  and window width  $t_W$  is at  $2 \text{ ps}$ .

#### 4. Conclusions

Systematic study of implementation of the Green–Kubo method for determination of the shear viscosity reveals the parameters that are most cost-effective. Because each independent component of the stress tensor enables one to compute an estimate of the shear viscosity, and because these values must, in a real fluid, converge to a single value,

a natural criterion of accuracy can be exploited. Using this metric, we studied the effect of simulation duration,  $t_D$ , width of the correlation window,  $t_W$  and the temporal spacing between time origins,  $t_s$ . We find that a set of optimal values that effectively trade off accuracy with computational cost are  $t_D = 2 \text{ ns}$ ,  $t_W = 2 \text{ ps}$  and  $t_s = 10 \text{ fs}$ . Although for different materials with different potential forms or parameters these specific temporal factors might

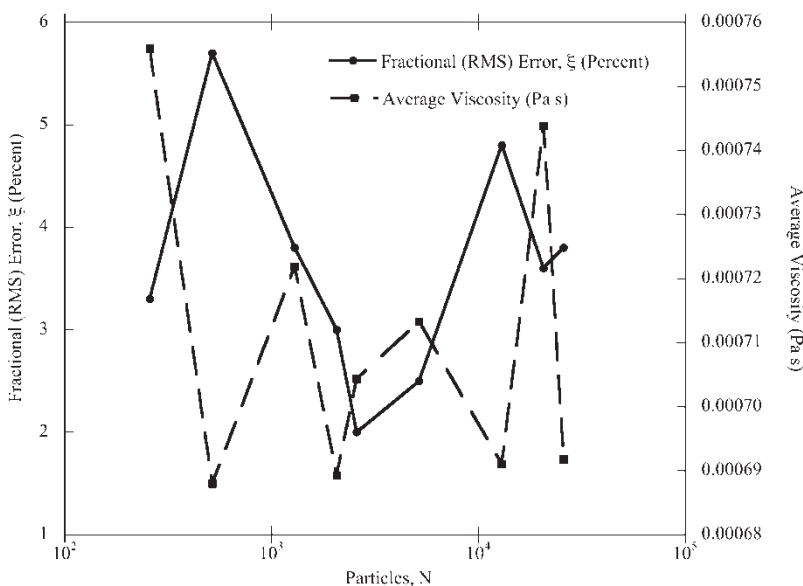


Figure 5. Fractional RMS error,  $\xi$  and average shear viscosity as a function of  $N$  (particle number) at  $1399 \text{ K} (\pm 79 \text{ K})$ ,  $182.4 \text{ MPa} (\pm 165.7 \text{ MPa})$  and  $\rho = 1379.3 \text{ kg m}^{-3}$ . Simulation duration  $t_D = 2 \text{ ns}$ ,  $t_W = 2 \text{ ps}$  and  $t_s = 10 \text{ fs}$  for all calculations. Although there is no obvious dependence of  $\xi$  on  $N$ , it should be emphasized that the fluctuation in temperature ( $\sigma_T$ ) and pressure ( $\sigma_P$ ) scale as  $N^{-1/2}$ . In order to assign a shear viscosity to a specific well-known temperature and pressure, large  $N$  simulations are required (figure 6).

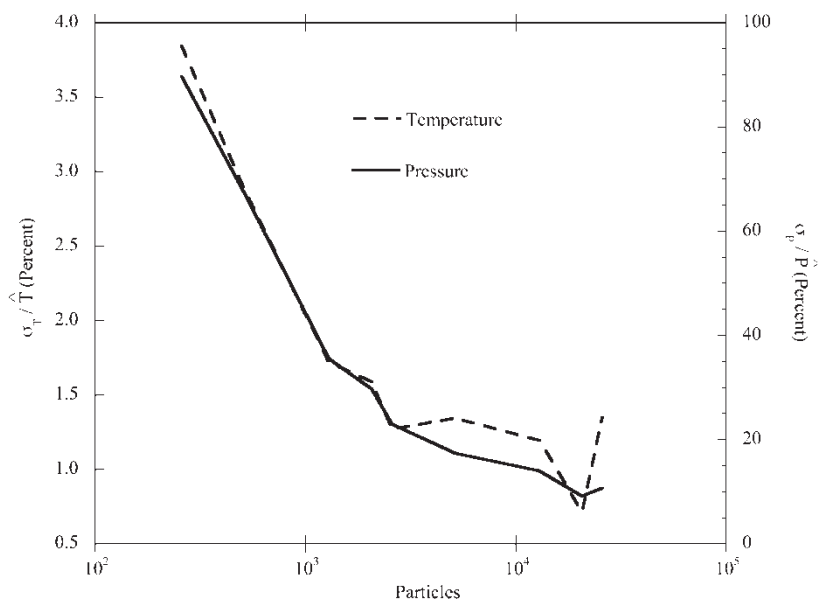


Figure 6. Normalized temperature ( $\sigma_T/\hat{T}$ ) and pressure ( $\sigma_P/\hat{P}$ ) fluctuations vs. particle number,  $N$ . In the limit of large  $N$ ,  $\sigma_T$  and  $\sigma_P$  scale as  $N^{-1/2}$ . Since, one must associate a shear viscosity to a specific state point, large  $N$  simulations are needed to decrease  $\sigma_T$  and  $\sigma_P$  to acceptable levels. Although the GK retrieval of shear viscosity does not depend explicitly upon  $N$ , the uncertainty of the state point T and P clearly do.

change, the methodology developed in this study remains [13]. Although  $\xi$  does not depend on the number of particles in the simulation, the fluctuations in temperature and pressure of the run, and hence the uncertainty of the state scale as  $N^{-1/2}$ . Hence, a viscosity computed by the GK method cannot be reliably placed in the context of material behaviour unless the state point is known well. This requires a relatively large number of particles.

## Acknowledgements

This research was supported by an allocation of advanced computing resources supported by the National Science Foundation and the Office of Science of the US Department of Energy. The computations were performed in part on DataStar at the San Diego Supercomputer Center and Seaborg at the National Energy Research Scientific Computing Center. We also thank Nuno Galamba, Toshiro Tanimoto Mark Ghiorso, and two anonymous reviewers for useful discussions on various parts of this work. We acknowledge support from NSF grants EAR-0440057 and ATM-0425059 and DOE grant DE-FG-03-91ER-14211 to FJS.

## References

- [1] S. Bastea. Transport properties of dense fluid argon. *Phys. Rev. E*, **68**, 031204 (2003).
- [2] Hiroshi Ogawa, Yutaka Shiraishi, Katsuyuki Kawamura, Toshio Yokokawa. Molecular dynamics study on the shear viscosity of molten  $\text{Na}_2\text{O}\cdot 2\text{SiO}_2$ . *J. Non-Cryst. Solids*, **119**, 2 (1990).
- [3] D.C. Rapaport. *The Art of Molecular Dynamics Simulation*, pp. 116–117 Cambridge University Press, Cambridge (1995).
- [4] Dario Alfe, Michael Gillan. First-principles calculation of transport coefficients. *Phys. Rev. Lett.*, **81**, 23 (1998).
- [5] G.J. Janz. Molten salts data as reference standards for density, surface tension, viscosity and electrical conductance:  $\text{KNO}_3$  and  $\text{NaCl}$ . *J. Phys. Chem. Ref. Data*, **9**, 4 (1980).
- [6] N. Galamba, C.A. Nieto de Castro, J.F. Ely. Molecular dynamics simulation of the shear viscosity of molten alkali halides. *J. Phys. Chem.*, **108**, 3658 (2004).
- [7] F.G. Fumi, M.P. Tosi. Ionic sizes and born repulsive parameters in the  $\text{NaCl}$ -type alkali halides-I. *J. Phys. Chem. Solids*, **25**, 31 (1964).
- [8] J.W.E. Lewis, K. Singer, L.V. Woodcock. Thermodynamic and structural properties of liquid ionic salts obtained by Monte Carlo computation. Part 2. Eight alkali metal halides. *J. Chem. Soc. Faraday Trans. 2*, **71**, 301 (1975).
- [9] S.J. Plimpton. Fast parallel algorithms for short-range molecular dynamics. *J. Comp. Phys.*, **117**, 1 (1995).
- [10] K. Refson. *Moldy User's Manual*, Oxford Department of Earth Sciences, Oxford (2001).
- [11] Y. Matsui, K. Kawamura, Y. Syono. Molecular dynamics calculations applied to silicate systems: molten and vitreous  $\text{MgSiO}_3$  and  $\text{Mg}_2\text{SiO}_4$  under low and high pressures. In *High Pressure Research in Geophysics: Advances in Earth and Planetary Sciences*, S. Akimoto, M.H. Manghnani (Eds.), pp. 511–524, Reidel, Boston, Massachusetts (1982).
- [12] D.A. McQuarrie. *Statistical Mechanics*, Harper Collins, New York (1976).
- [13] M.S. Ghiorso, D. Nevins, F.J. Spera. Molecular Dynamics Studies of  $\text{MgSiO}_3$  Liquid to 150 GPa: An Equation of State (EOS), Tracer Diffusivities, and a Detailed Analysis of Changes in Atomic Coordination Statistics as a Function of Temperature and Pressure. *Eos Trans. AGU*, **87**(52) (2006) Fall Meet. Suppl., Abstract MR43B-1079.